Kinetic and equilibrium studies on the adsorption of Direct Red 23 dye from aqueous solution using montmorillonite nanoclay

Amir Hossein Mahvi and Arash Dalvand

ABSTRACT

In this research, the adsorption of the Direct Red 23 dye from synthetic textile wastewater using nanoclay was studied in a batch system. The properties of nanoclay were investigated by scanning electron microscope, Fourier transform infrared, and EDX analysis. The specific surface area of the nanoclay was determined using Sear's method. The results revealed that with increasing adsorbent dose and contact time and decreasing pH, ionic strength, and adsorbate concentration, dye removal efficiency has increased. Nanoclay could remove 99.4% dye from the solution containing 50 mg/L dye at 30 min. The results indicated that dye removal followed pseudo-second-order kinetic ($R^2 > 0.99$) and the Langmuir isotherm. According to the findings, nanoclay is an effective adsorbent for direct dye removal from wastewater.

Key words | adsorption, direct dye, isotherms, kinetics, nanoclay

Amir Hossein Mahvi
Department of Environmental Health Engineering, School of Public Health,
Tehran University of Medical Sciences,
Tehran,
Iran;
Center for Solid Waste Research, Institute for Environmental Research,
Tehran University of Medical Sciences,
Tehran, Iran
and
National Institute of Health Research,
Tehran University of Medical Sciences,
Tehran, Iran

Arash Dalvand (corresponding author)
Environmental Science and Technology Research Center, Department of Environmental Health Engineering, School of Public Health,
Shahid Sadoughi University of Medical Sciences,
Yazd, Iran
E-mail: *arash.dalvand@gmail.com*

INTRODUCTION

Textile industries generate a high volume of colored wastewater containing various synthetic dyes and pigments (Mahmoodi & Dalvand 2013; Dalvand *et al.* 2017). The presence of a little amount of dyes in water is highly visible (Maleki *et al.* 2010). Discharge of colored textile wastewater in water bodies is harmful to aquatic organisms and imposes serious damage to the environment (Kizilkaya 2012; Yousefi *et al.* 2017). Some synthetic dyes are toxic, carcinogenic, or mutagenic (Dalvand *et al.* 2011, 2016; Ashrafi *et al.* 2013; Vu *et al.* 2019). Because of the low biochemical oxygen demand (BOD)/chemical oxygen demand (COD) ratio of textile wastewater (Amin *et al.* 2008), and the existence of polyaromatic compounds in the structure of synthetic dyes (Christie 2007), common wastewater treatment methods, such as biological processes (conventional activated sludge process), are not applicable for the efficient treatment of textile wastewater (Mahvi *et al.* 2009; Gholami-Borujeni *et al.* 2011). Adsorption method due to advantages, such as high speed to remove contaminants, simplicity of design, easy operation, and high efficiency to remove pollutants (Mahvi 2008; Shirmardi *et al.* 2013; Palamthodi & Lele 2016; Dalvand *et al.* 2018), in recent years, has been widely employed to remove pollutants, such as arsenic (Zarei *et al.* 2017), chromium (Aslani *et al.* 2018), lead (Khazaei *et al.* 2018), malachite green (Kooh *et al.* 2018), methyl orange dye (Min-Yu & Su-Hsia 2006), methylene blue and crystal violet (Chahm *et al.* 2018), and fluoride (Kaygusuz *et al.* 2015) from water and wastewater.

Although activated carbon is the most widely used adsorbent in water and wastewater treatment (Min-Yu & Su-Hsia 2006), it has some disadvantages, such as high cost and needs to regenerate, which limit its application for the removal of pollutants from water and wastewater (Almeida *et al.* 2009). To overcome these limitations, in recent years, uses of new and low-cost adsorbents, such as sawdust (Hebeish *et al.* 2011), orange peel (Arami *et al.* 2005), and clay

doi: 10.2166/wqrj.2019.008

(Min-Yu & Su-Hsia 2006; Moharami & Jalali 2013), to remove pollutants from the aqueous environment have been increased.

Nanoclay is nanoparticles of layered mineral silicates (Niroumand *et al.* 2013), which is one of the cheapest nanomaterials that possesses properties such as being non-toxic to the environment, high specific surface area, high adsorption capacity, and high surface reactivity and stability (Jamshidi *et al.*2014; Salam *et al.* 2017). In recent years, nanoclay has been successfully applied for the removal of phosphorus (Yuan & Wu 2007), Orange G dye (Salam *et al.* 2017), copper, and mercury (Soleimani & Siahpoosh 2015) from water and wastewater.

Direct Red 23 (DR 23) is an anionic dye (Arami *et al.* 2005) which contains two anionic sulfonate groups. This dye is not biodegradable and has a carcinogenic nature (Konicki *et al.* 2012). The DR 23 dye is widely used for dyeing textile fibers.

Until now, no studies have been conducted on the adsorption of DR 23 by nanoclay. Thus, the main objective of this study was to investigate the removal of DR 23 from synthetic textile wastewater by using nanoclay. The effects of parameters, such as pH, ionic strength, adsorbent dose, contact time, and adsorbate concentration on dye removal efficiency, were investigated. In addition, kinetics and isotherms of adsorption were studied.

MATERIALS AND METHODS

Materials

DR 23 was obtained from Ciba Company and applied without further purification. It was selected as the model dye since it was widely used for dyeing fibers by Iranian textile industries. The properties of DR 23 are given in Table 1. Direct Red 80 (chemical formula: $C_{45}H_{26}N_{10}Na_6O_{21}S_6$, molecular weight: 1,373 g/mol, λmax: 537 nm) was purchased from Ciba. The montmorillonite nanoclay was purchased from the Nanosav Company (Iran). According to the supplier information, the density and the interlayer spacing of nanoclay sheets were 0.6 g/cm^3 and 5 nm, respectively. NaCl, NaOH, and HCl were obtained from the Merck Company (Germany).

Adsorption experiments

For conducting of adsorption tests, each 100 ml Erlenmeyer glass flask was filled with 50 ml of synthetic wastewater containing a specific amount of dye (10–200 mg/L). A certain dose of adsorbent (0.5–5 g/L) was measured and added to each flask and pH was adjusted to 2, 3, 4, 5, 6, 7, 8, 9, 10, or 11, and the mixture was shaken at 250 rpm for specific times (2–150 min). After shaking, samples were filtered using a 0.45 μm filter to separate adsorbent from the solution, and the solution was analyzed by a spectrophotometer to detect residual dye. All experiments were done at room temperature (25 °C).

Analytical methods

Dye concentration was determined at the maximum wavelength (505 nm) using a UV–Vis spectrophotometer (Perkin Elmer, lambda 25, USA). For adjusting the pH, 0.1 M NaOH and 0.1 M HCl were used. pH meter (Kent Ell 7020, UK) was used for pH measurement.

Table 1 | Properties of DR 23

Dye	C.I. DR 23
Chemical structure	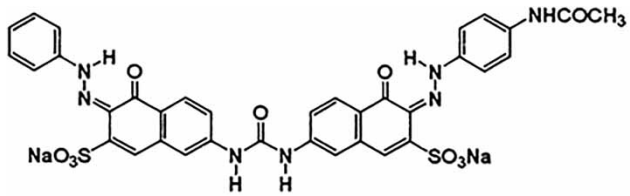
Chemical formula	$C_{35}H_{25}N_7Na_2O_{10}S_2$
Molecular weight (g/mol)	813.7
λmax (nm)	505

To understand the morphology of the adsorbent, the image of nanoclay was recorded using a scanning electron microscope (SEM) (AIS2300, Seron Technology, South Korea) at an accelerating voltage of 20 kV. For recording the infrared spectrum of nanoclay, a Fourier transform infrared (FTIR) spectrometer (Perkin Elmer, USA) was applied.

The percentage of dye removal was determined according to Equation (1):

$$\eta = \frac{(C_0 - C)}{C_0} \times 100 \quad (1)$$

where η is dye removal (%) and C_0 and C are dye concentrations before and after adsorption (mg/L), respectively.

The amount of dye adsorbed onto the adsorbent at equilibrium was calculated using the following equation (Palamthodi & Lele 2016; Yuliani *et al.* 2017):

$$q_e = \frac{(C_0 - C_e)V}{m} \quad (2)$$

where q_e is adsorption capacity (mg/g), C_0 and C_e are initial and equilibrium concentrations of dye in solution (mg/L), V is the volume of solution (L), and m is the mass of the adsorbent (g).

Specific surface area

Sear's method was used to measure the specific surface area of the nanoclay (Dada *et al.* 2012). A total of 0.5 g nanoclay was added to 50 ml of 0.1 M HCl on a magnetic stirrer, and 10 g NaCl was poured into the solution. The resulting mixture was titrated using standard 0.1 M NaOH in a water bath at 298 K to pH 4, and then to pH 9. The specific surface area was determined by Equation (3):

$$S = 32V - 25 \quad (3)$$

where S (m^2/g) and V (ml) are the specific surface area and the volume of NaOH required to raise the pH from 4 to 9, respectively.

RESULTS AND DISCUSSION

Characteristics of nanoclay

The morphology of nanoclay was characterized using an SEM. Figure 1 shows that nanoclay has a layered structure, smooth surface, and the presence of a number of asymmetric open pores in the adsorbent provides a large area for the adsorption of dye molecules. According to the result obtained from Sear's method, the specific surface area of nanoclay was 55 m^2/g.

Figure 2 depicts the FTIR spectra of nanoclay. The peak at 3,622 cm^{-1} is related to the O-H group. The bands at 3,426 and 1,636 cm^{-1} are attributed to H-O-H molecules of water adsorbed on the mineral. Two peaks at 914 and

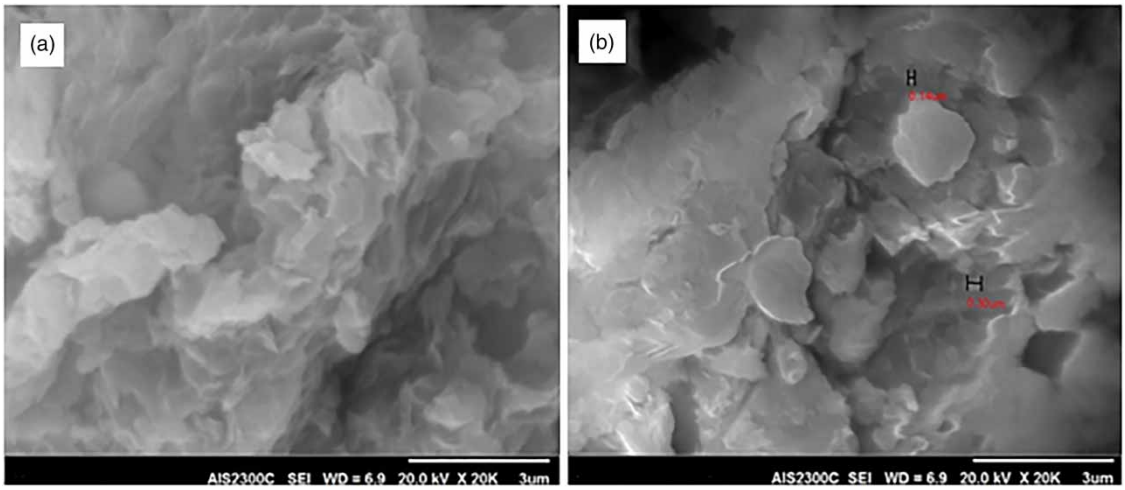

Figure 1 | SEM images of nanoclay surface (magnification: 20 kx).

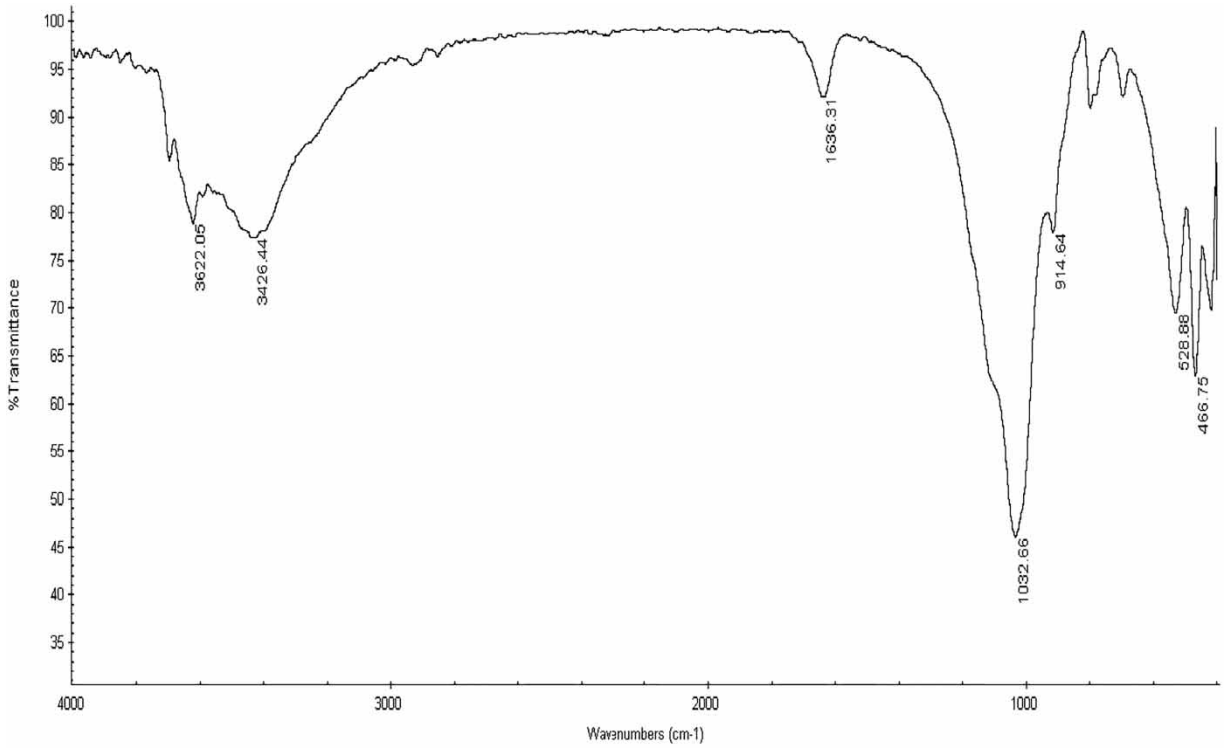

Figure 2 | FTIR spectra of nanoclay.

1,032 cm^{-1} are ascribed to aluminol (Al-OH_2) and silanol (Si-O) groups, respectively (Feng *et al.* 2000). The bands at 466 and 528 cm^{-1} indicate the presence of Si-O-Si and Si-O-Al in the structure of montmorillonite nanoclay.

The elemental analysis maps for Al, Si, O, Fe, Na, Mg, Ca, and K, and EDX spectra of nanoclay are given in Figure 3. Figure 3 confirms the complete dispersion of all elements in the structure of nanoclay. According to the EDX spectra (Figure 3(i)), the nanoclay was majorly comprised of 10.44% Al, 32.78% Si, 47.08% O, 5.53% Fe, 0.79% Na, 1.32% Mg, 1.56% Ca, and 0.5% K.

Effect of contact time

It has been proven that enough contact time provides an opportunity for interaction between the adsorbate and the adsorbent (Hebeish *et al.* 2011). To determine the effect of contact time on dye removal by nanoclay at various doses (0.5, 2, and 5 g/L) and the initial dye concentration of 50 mg/L, according to pretest, different time intervals (2, 5, 10, 20, 30, 40, 50, 60, 90, 120, and 150 min) were chosen and the results are presented in Figure 4. This figure shows that with increasing contact time, dye removal efficiency increases and the highest dye removal efficiency and adsorption capacity were obtained after 30, 60, and 120 min for adsorbent doses of 5, 2, and 0.5 g/L, respectively. As it is clear from the results, dye removal is rapid in the initial stages of sorption and then becomes slow and eventually depending on the adsorbent dose achieves to equilibrium at a specific time (Hassan *et al.* 2014). By increasing the adsorbent dose from 0.5 to 5 g/L, the required time to reach equilibrium decreases. In the first stage of adsorption, many vacant sites are available and adsorption is fast (Weber *et al.* 2014), but later due to occupying and decreasing vacant sites, driving force decreases that lead to a decrease in the rate of adsorption (Yan *et al.* 2013). These results are in agreement with the results reported by Hebeish *et al.* (2011).

Effect of adsorbent dose

In order to assess the effect of the adsorbent dose on DR 23 dye removal efficiency and adsorption capacity, eight adsorbent doses (0.5, 1, 1.5, 2, 3, 4, and 5 g/L) were tested, while other

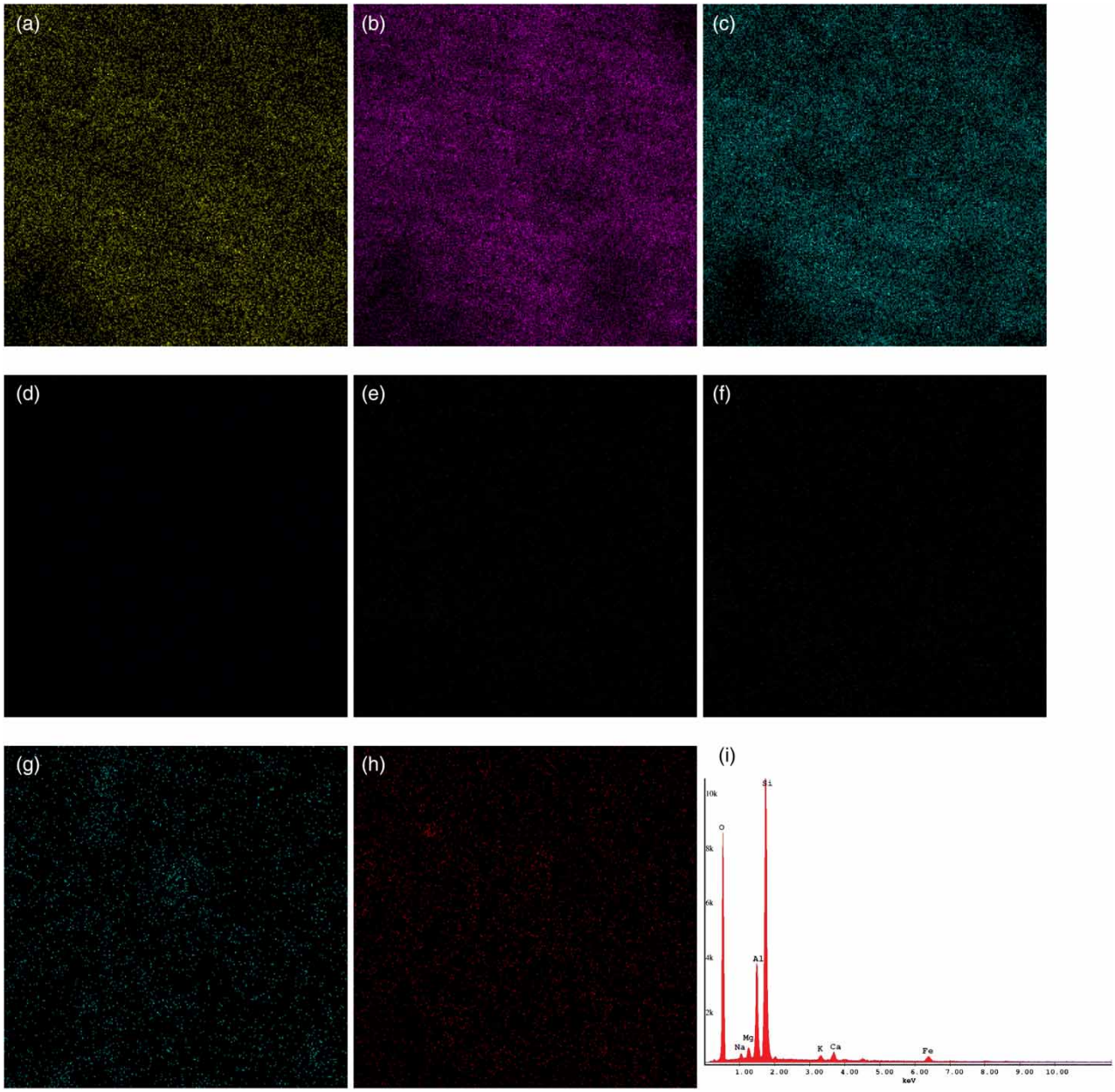

Figure 3 | Elemental analysis maps for (a) AL, (b) Si, (c) O, (d) Mg, (e) Na, (f) Fe, (g) K, (h) Ca, and (i) the EDX spectra of nanoclay.

parameters were kept constant (pH: 2, time: equilibrium time, and dye concentration: 50 and 200 mg/L) and the results are shown in Figure 5. As it can be seen in this figure, the increase of dye removal from 82.26 to 99.4% and from 46.25 to 97%, at initial dye concentrations of 50 and 200 mg/L, by increasing the adsorbent dose from 0.5 to 5 g/L is due to the increment of the surface area and the availability of more vacant sites for adsorption (Abdel-Halim & Al-Deyab 2011; Hebeish *et al.* 2011). In this study, the efficiency of nanoclay for the removal of Direct Red 80 dye was also investigated, and the results showed that with increasing the adsorbent dose from 0.5 to 5 g/L at initial dye concentrations of 50 and 200 mg/L, the dye removal efficiency enhanced from 16.7 to 92.4% and from 5.9 to 73.4%, respectively.

Figure 5 shows that the adsorption capacity decreases from 81.26 to 9.94 mg/g by increasing adsorbent doses

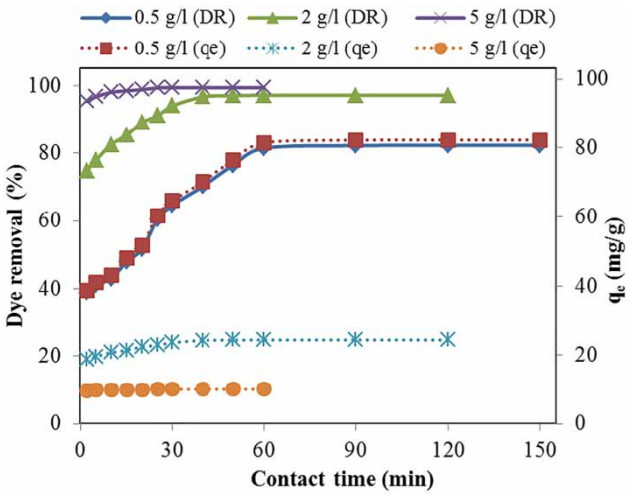

Figure 4 | Effect of contact time on DR 23 dye removal (dye concentration: 50 mg/L; adsorbent dose: 0.5, 2, and 5 g/L; and pH: 2).

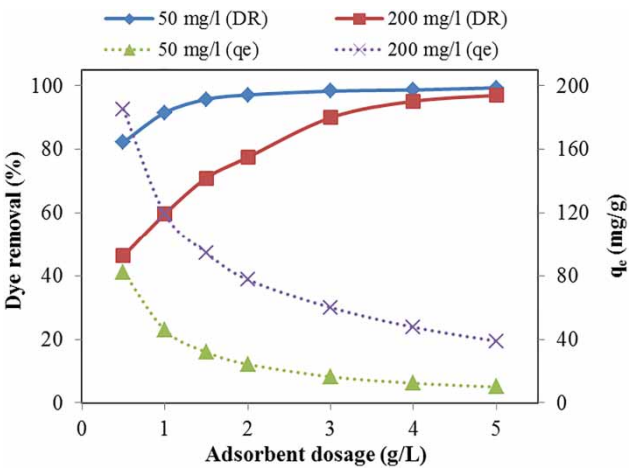

Figure 5 | Effect of the adsorbent dose on DR 23 dye removal (dye concentrations: 50 and 200 mg/L and pH: 2).

from 0.5 to 5 g/L. These results could be attributed to overcrowding of the adsorbent particles that result in the overlapping or aggregation of the adsorption sites, reducing the available surface area and an increase in the diffusion path length (Hebeish *et al.* 2011). Similar results have been observed by Mahmoodi *et al.* (2011).

Effect of pH

The initial pH of the aqueous solution is an important parameter that influences the adsorption process (Almeida *et al.* 2009) by controlling the surface charge of the adsorbent, the adsorption availability of the dyes, and the degree of ionization of the atoms or molecules in the solution (Errais *et al.* 2011). The effect of solution pH on the dye removal efficiency and adsorption capacity was evaluated at pH 2–11 (Figure 6). According to Figure 6, by increasing pH from 2 to 11, a decrease in the dye removal efficiency and adsorption capacity was observed. At all adsorbent doses, maximum dye removal was achieved at pH 2. At low pH, the aluminol and silanol groups on the nanoclay surface were protonated in the form of $AlOH_2^+$ (Bajpai & Sachdeva 2002) and $SiOH_2^+$ ($\equiv Si–OH + H^+ \rightarrow \equiv Si–OH_2^+$) (Kubilay *et al.* 2007) due to the presence of excess H^+ ions in the solution. Higher dye removal efficiency at pH 2 can be attributed to the protonation of active groups on the surface of the adsorbent, which improves the electrostatic attraction of negatively charged dye molecules (each dye molecule contains two anionic sulfonate groups) toward positively charged adsorbent (Konicki *et al.* 2012). With increasing pH, due to the deprotonation mechanism (AlOH and SiOH change to AlO^- and SiO^-), the number of positively charged sites on the adsorbent decreases and as a result the dye removal efficiency decreases (Si *et al.* 2015). Moreover, lower dye adsorption at higher pH is because of the presence of negatively charged hydroxyl ions which compete with the anionic dye molecules for the adsorption sites (Gopal *et al.* 2014).

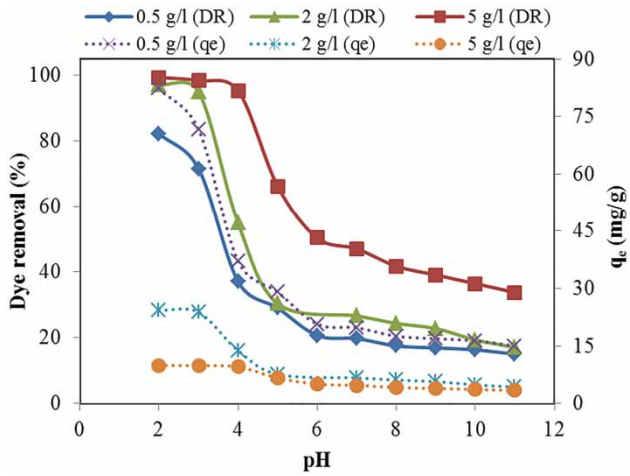

Figure 6 | Effect of pH on DR 23 dye removal (dye concentration: 50 mg/L; adsorbent dose: 0.5, 2, and 5 g/L; and contact time: equilibrium time).

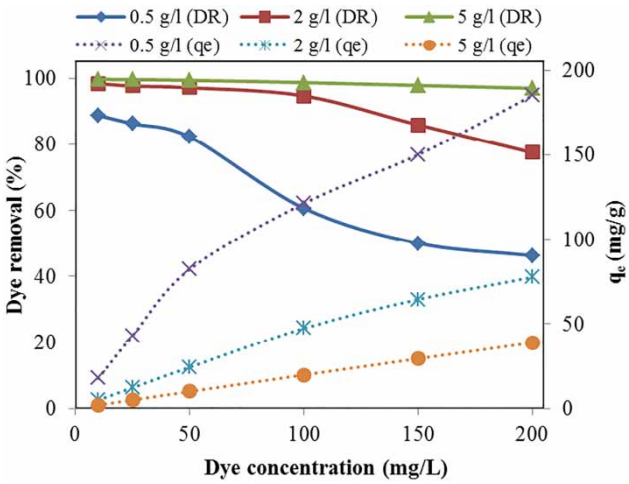

Figure 7 | Effect of initial dye concentration on DR 23 dye removal (adsorbent dose: 0.5, 2, and 5 g/L and pH: 2).

Effect of adsorbate dose

The initial concentration of the adsorbate in solution supplies an important driving force to overcome the mass transfer resistance between the solution and the solid adsorbent (Almeida *et al.* 2009). The influence of adsorbate concentration on adsorption efficiency was studied at various initial DR 23 dye concentrations, while other parameters were kept fixed (pH: 2, contact time: equilibrium time, and adsorbent dose: 0.5, 2, and 5 g/L). Figure 7 shows all adsorbent doses when the initial dye concentration increases, the percentage of dye removal decreases, but adsorption capacity improves. With an increase in initial DR 23 dye concentration from 10 to 200 mg/L, dye removal efficiency decreases from 88.79, 98.4, and 99.7% to 46.2,

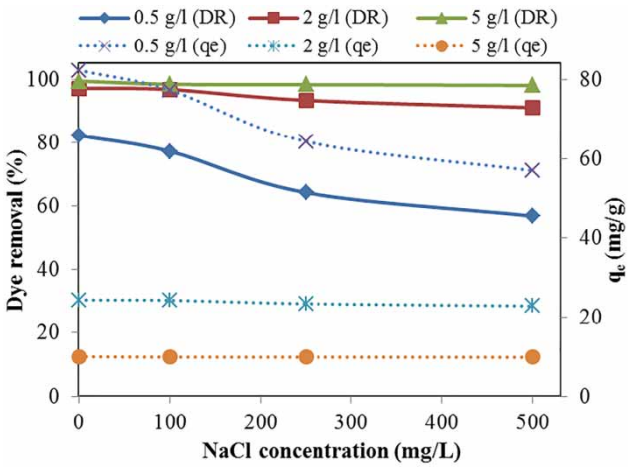

Figure 8 | Effect of NaCl concentration on DR 23 dye removal (dye concentration: 50 mg/L; adsorbent dose: 0.5, 2, and 5 g/L; contact time: equilibrium time; and pH: 2).

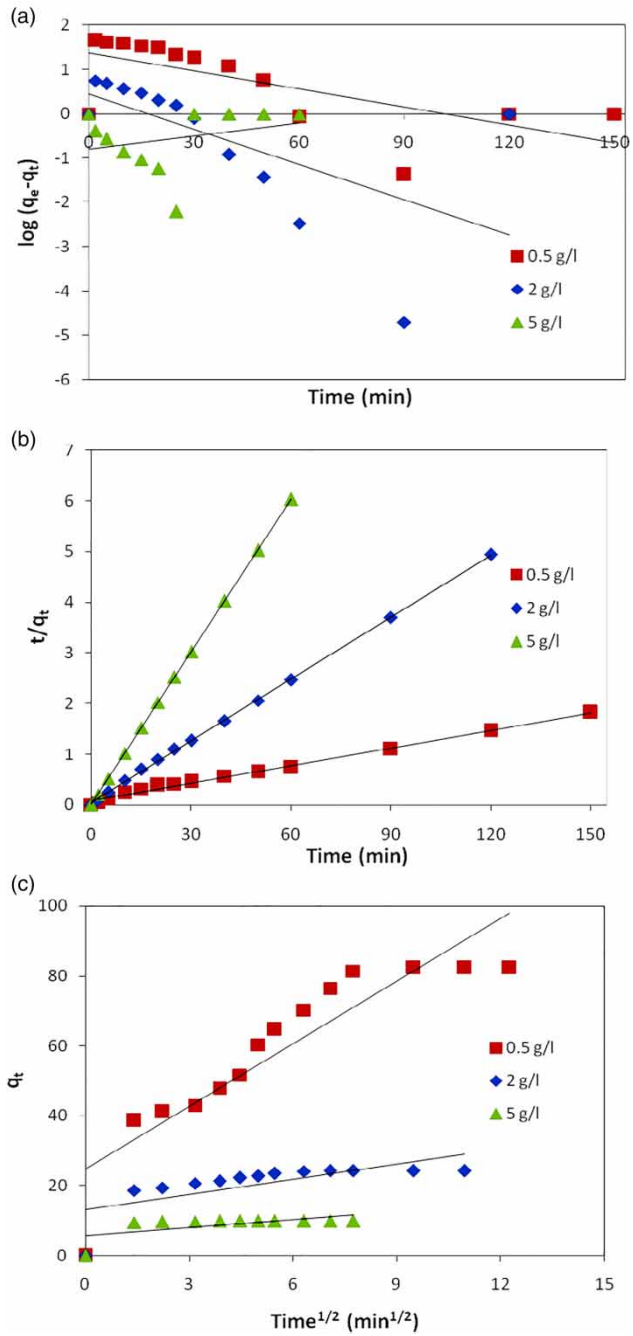

Figure 9 | (a) Pseudo-first-order, (b) pseudo-second-order, and (c) intraparticle diffusion kinetics for the adsorption of DR 23 onto nanoclay (dye concentration: 50 mg/L; adsorbent dose: 0.5, 2, and 5 g/L; and pH: 2).

77.5, and 97% at adsorbent doses of 0.5, 2, and 5 g/L, respectively. The effect of adsorbate dose on dye removal efficiency was also studied for the Direct Red 80 dye, and the results indicate that with increasing Direct Red 80 dye concentration from 10 to 200 mg/L, dye removal efficiency declines from 38.9 and 98% to 5.9 and 73.48% at adsorbent doses of 0.5 and 5 g/L, respectively.

This result can be explained by the fact that the number of adsorption sites on a specific amount of adsorbent is limited (Si *et al.* 2015); therefore, with increasing the number of dye molecules, the number of active sites on the adsorbent is not enough to adsorb all dye molecules and, consequently, dye removal decreases. By increasing the initial DR 23 dye concentration from 10 to 200 mg/L, the amount of dye adsorbed onto the adsorbent increased from 17.7, 4.9, and 1.99 mg/g to 185, 77.5, and 38.8 mg/g at adsorbent doses of 0.5, 2, and 5 g/L, respectively. An increase in the concentration gradient between dye molecules in the solution and dye molecules on the adsorbent surface at higher initial dye concentrations causes an increase in the driving force and adsorption capacity (Gopal *et al.* 2014).

Effect of competing ion

The high concentration of salts (especially NaCl) in common textile wastewater can affect the adsorption of pollutants onto the adsorbent (Si *et al.* 2015). To investigate the effect of the competing ion on dye adsorption, NaCl in different concentrations of 100, 250, and 500 mg/L was added to textile wastewater (Figure 8). As is clear from Figure 8, increasing NaCl concentration from 0 to 500 mg/L results in decreasing dye removal at all adsorbent doses. This result is due to the presence of salt molecules in adsorption sites on the surface of the adsorbent (Mahmoodi *et al.* 2011), and the competition of chloride ions with DR 23 dye molecules for adsorption sites on the adsorbent surface (Errais *et al.* 2011). At a high adsorbent dose, when NaCl was added to the solution, only a negligible decrease in dye adsorption by the adsorbent was observed. The low decrease in dye removal at higher adsorbent doses is due to the presence of enough available active sites for the adsorption of both dye and salt molecules.

Adsorption kinetics

Until now, many kinetic models have been presented for investigating the rate of adsorption process (Gopal *et al.* 2014). In the current study, the kinetics of dye adsorption onto nanoclay was assayed by pseudo-first-order (Lagergren 1898; Mahmoodi & Masrouri 2015), pseudo-second-order (Ho & McKay 1998; Magdy & Altaher 2018), and intraparticle diffusion models (Weber & Morris 1963) (Figure 9). The intraparticle diffusion model assumes that diffusion is the only rate-controlling step during the adsorption process (Öztürk & Malkoc 2014).

The kinetic parameters for dye adsorption onto nanoclay are presented in Table 2. The values of C (Table 2) showed that increasing the adsorbent dose decreased the boundary layer diffusion effect. According to the correlation

Table 2 | Kinetic parameters for dye adsorption onto the adsorbent (pH: 2 and adsorbent dose: 0.5, 2, and 5 g/L)

			Adsorbent dose (g/L)		
Kinetic model	**Linear form of equation**	**Kinetic coefficient**	**0.5**	**2**	**5**
Pseudo-first-order	$\log(q_e - q_t) = \log q_e - \frac{k_1 t}{2.303}$	k_1 (min^{-1})	0.03	0.059	0.002
		R^2	0.458	0.37	0.077
Pseudo-second-order	$\frac{t}{q_t} = \frac{t}{k_2 q_e^2} + \frac{t}{q_e}$	k_2 (g/mg min)	0.0014	0.031	1
		$q_{e,\text{calculated}}$ (mg/g)	90.9	25	10
		h	11.49	19.6	100
		R^2	0.993	0.999	1
Intraparticle diffusion	$q_t = k_{id} t^{1/2} + C$	k_{id} (mg/g $min^{1/2}$)	5.978	1.449	0.76
		C (mg/g)	24.8	13.27	5.71
		R^2	0.819	0.489	0.38

coefficient from Table 2, the adsorption data were best fitted to the pseudo-second-order model at various adsorbent doses ($0.993 < R^2 < 1$). Also, the values of q_e calculated using the pseudo-second-order model were near to q_e gathered from experimental results. The values of q_e experimental were 82.26, 24.29, and 9.94 mg/g for adsorbent doses of 0.5, 2, and 5 g/L, respectively. Although with an increase in the adsorbent dose from 0.5 to 5 g/L the q_e parameter decreases, the rate of reaction increases from 0.001 to 1 g/mg min. These results agree with the results reported by previous studies (Mahmoodi *et al.* 2011; Gopal *et al.* 2014). At higher adsorbent doses, more adsorption sites are available; hence, the adsorption process is completed in a short time, and the rate of reaction (k_2) increases.

Adsorption isotherms study

The adsorption capacity of any adsorbent can be computed by using a suitable isotherm model (Almeida *et al.* 2009). In this study, Langmuir (1916), Freundlich (1906), and Dubinin–Radushkevich (Dubinin 1947) models were selected for studying the adsorption isotherm (Figure 10), and adsorption parameters are shown in Table 3. The Langmuir isotherm describes the monolayer and homogeneous sorption of pollutants on the surface of the adsorbent (Kaygusuz *et al.* 2015), while the Freundlich model assumes that the adsorption of pollutants on the adsorbent is multilayer and heterogeneous. The results presented in Table 3 indicated that DR 23 dye removal followed the Langmuir isotherm ($R^2 > 0.99$).

The value of n above 1 suggests that the adsorption of DR23 onto nanoclay is favorable and indicates the presence of high energy sites on the adsorbent surface (Ratnamala *et al.* 2012). To determine the nature of adsorption (physical or chemical), the Dubinin–Radushkevich model was also used (Ghaedi *et al.* 2015). The value of mean sorption energy (E) can give useful information about the nature of adsorption. The value of $E < 8$ kJ/mol indicates physical adsorption. When the value of E ranges from 8 to 16 kJ/mol, the adsorption process follows chemical ion exchange. According to Table 3, the values of E for the adsorption of DR 23 onto nanoclay are 0.79, 2.236, and 3.535 kJ/mol for initial adsorbent doses of 0.5, 2, and 5 g/L; therefore, the nature of dye adsorption onto nanoclay is physical.

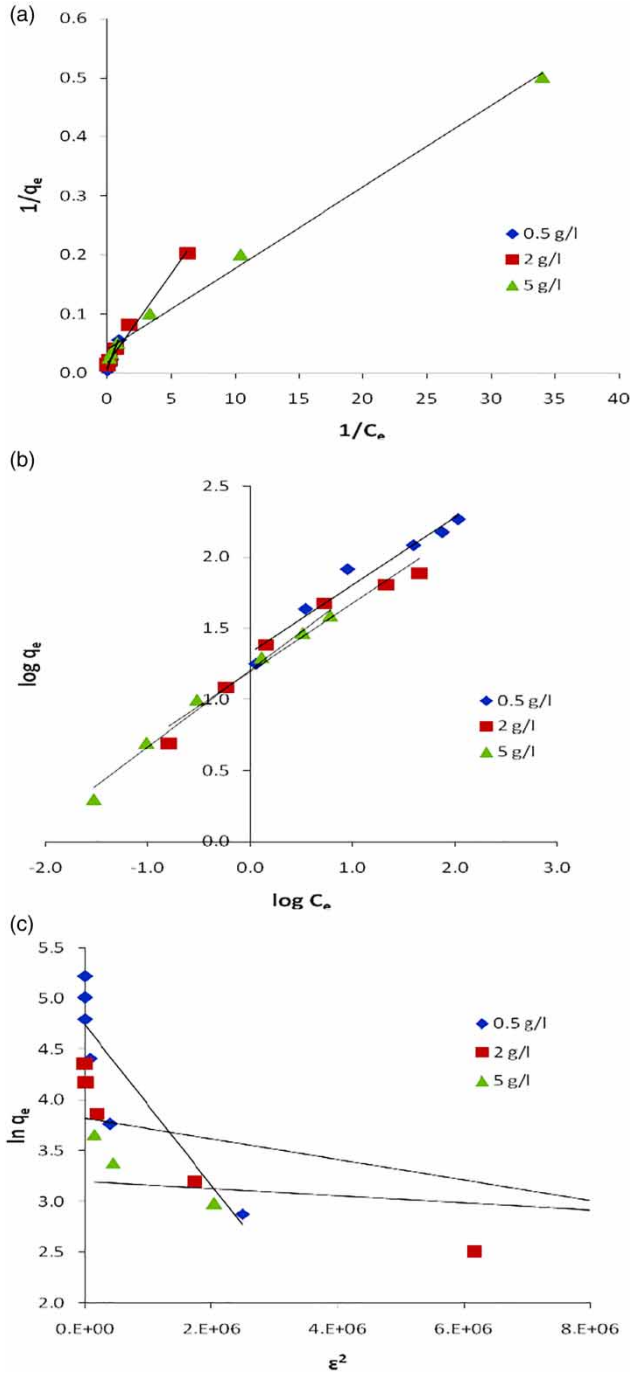

Figure 10 | (a) Langmuir, (b) Freundlich, and (c) Dubinin–Radushkevich isotherms for the adsorption of DR 23 onto nanoclay (adsorbent dose: 0.5, 2, and 5 g/L, and pH: 2).

Comparison of nanoclay with other adsorbents

Nanoclay has been compared with other adsorbents for DR 23 dye adsorption (Table 4). The results in this table show

Table 3 | Isotherm parameters for dye adsorption onto the adsorbent (pH: 2, contact time: equilibrium time, and adsorbent dose: 0.5, 2, and 5 g/L)

			Adsorbent dose (g/L)		
Adsorption isotherm	**Linear form of equation**	**Isotherm coefficient**	**0.5**	**2**	**5**
Langmuir	$\frac{1}{q_e}=\frac{1}{q_{\max}}+\frac{1}{bq_{\max}}\frac{1}{C_e}$	$q_{\max}$ (mg/g)	166.6	58.82	25.64
		b (L/mg)	0.107	0.566	3
		R^2	0.998	0.992	0.994
Freundlich	$\log q_e=\log k_f+\frac{1}{n}\log C_e$	k_f (mg/g)(L/mg)$^{1/n}$	21.42	15.66	16.18
		n	2.1	2.07	1.84
		R^2	0.95	0.947	0.987
Dubinin–Radushkevich	$\ln q_e=\ln q_m-\beta\varepsilon^2$	β (mol^2/J^2)	8×10^{-7}	10^{-7}	4×10^{-8}
		q_m (mg/g)	114.2	45.51	24.41
		E (kJ/mol)	0.79	2.236	3.535
	$E=\frac{1}{(2\beta)^{1/2}}$	R^2	0.787	0.801	0.904

Table 4 | Comparison of the various adsorbents for DR 23 removal

Adsorbent	**Maximum adsorption capacity (mg/g)**	**pH**	**Applicable kinetic model**	**Applicable isotherm model**	**Reference**
Cationized sawdust	65.8	5.5	–	Langmuir	Hebeish *et al.* (2011)
Polyaniline coated activated carbon	90.9–109.8	3	Pseudo-second-order	Langmuir	Gopal *et al.* (2014)
Magnetic multi-walled carbon nanotubes-Fe_3C	172.4	3.7	Pseudo-second-order	Freundlich	Konicki *et al.* (2012)
Chitosan	155	2	Pseudo-second-order	Temkin	Mahmoodi *et al.* (2011)
Corn stalk	27–52	3	Pseudo-second-order	Freundlich	Fathi *et al.* (2015)
Orange peel	10.72	2	Pseudo-second-order	Langmuir	Arami *et al.* (2005)
Uncariagambir	26.67	2	Pseudo-second-order	Langmuir	Achmad *et al.* (2012)
Pretreated Mangrove bark	21.55	2	Pseudo-second-order	Langmuir	Tan *et al.* (2010)
Zinc aluminum hydroxide	75	–	Pseudo-second-order	Langmuir	Mahmoodi *et al.* (2014)
Nanoclay	25–166	2	Pseudo-second-order	Langmuir	This study

that pH 2 is the most desirable pH for DR 23 adsorption. The adsorption of DR 23 onto the whole of adsorbents has followed the pseudo-second-order model. Compared to other low-cost adsorbents (corn stalk, orange peel, Mangrove bark, sawdust, and Uncariagambir), nanoclay has a higher capability for DR 23 removal. In addition, nanoclay in price and adsorption capacity can compete well with modified adsorbents and other nano-adsorbents.

CONCLUSION

The adsorption of DR 23 onto nanoclay was studied at different conditions. The results revealed that by increasing the adsorbent dose and contact time and decreasing the pH, ionic strength, and adsorbate concentration, DR 23 dye removal efficiency has increased. Nanoclay could remove DR 23 from aqueous solution as high as 99.4%. The equilibrium data were fitted well with the Langmuir isotherm. Kinetic studies revealed that dye removal onto adsorbent followed the pseudo-second-order model. The nature of dye adsorption onto nanoclay was physical. It was found that nanoclay was an efficient adsorbent for direct dye removal from textile wastewater.

ACKNOWLEDGEMENT

The authors would like to thank the Tehran University of Medical Sciences and the Shahid Sadoughi University of Medical Sciences for supporting the research.

REFERENCES

Abdel-Halim, E. & Al-Deyab, S. S. 2011 Removal of heavy metals from their aqueous solutions through adsorption onto natural polymers. *Carbohydrate Polymers* **84** (1), 454–458.

Achmad, A., Kassim, J., Suan, T. K., Amat, R. C. & Seey, T. L. 2012 Equilibrium, kinetic and thermodynamic studies on the adsorption of direct dye onto a novel green adsorbent developed from Uncaria Gambir extract. *Journal of Physical Science* **23** (1), 1–13.

Almeida, C., Debacher, N., Downs, A., Cottet, L. & Mello, C. 2009 Removal of methylene blue from colored effluents by adsorption on montmorillonite clay. *Journal of Colloid and Interface Science* **332** (1), 46–53.

Amin, H., Amer, A., Fecky, A. & Ibrahim, I. 2008 Treatment of textile wastewater using H_2O_2/UV system. *Physicochemical Problems of Mineral Processing* **42**, 17–28.

Arami, M., Limaee, N. Y., Mahmoodi, N. M. & Tabrizi, N. S. 2005 Removal of dyes from colored textile wastewater by orange peel adsorbent: equilibrium and kinetic studies. *Journal of Colloid and Interface Science* **288** (2), 371–376.

Ashrafi, S. D., Rezaei, S., Forootanfar, H., Mahvi, A. H. & Faramarzi, M. A. 2013 The enzymatic decolorization and detoxification of synthetic dyes by the laccase from a soil-isolated ascomycete, *Paraconiothyrium variabile*. *International Biodeterioration & Biodegradation* **85**, 173–181.

Aslani, H., Kosari, T. E., Naseri, S., Nabizadeh, R. & Khazaei, M. 2018 Hexavalent chromium removal from aqueous solution using functionalized chitosan as a novel nano-adsorbent: modeling and optimization, kinetic, isotherm, and thermodynamic studies, and toxicity testing. *Environmental Science and Pollution Research* **25** (20), 20154–20168.

Bajpai, A. & Sachdeva, R. 2002 Study on the adsorption of hemoglobin onto bentonite clay surfaces. *Journal of Applied Polymer Science* **85** (8), 1607–1618.

Chahm, T., Martins, B. A. & Rodrigues, C. A. 2018 Adsorption of methylene blue and crystal violet on low-cost adsorbent: waste fruits of *Rapanea ferruginea* (ethanol-treated and H_2SO_4-treated). *Environmental Earth Sciences* **77** (13), 508.

Christie, R. 2007 *Environmental Aspects of Textile Dyeing*. Elsevier, Amsterdam.

Dada, A., Olalekan, A., Olatunya, A. & Dada, O. 2012 Langmuir, Freundlich, Temkin and Dubinin–Radushkevich isotherms studies of equilibrium sorption of Zn^{2+} unto phosphoric acid modified rice husk. *Journal of Applied Chemistry* **3** (1), 38–45.

Dalvand, A., Gholami, M., Joneidi, A. & Mahmoodi, N. M. 2011 Dye removal, energy consumption and operating cost of electrocoagulation of textile wastewater as a clean process. *Clean – Soil, Air, Water* **39** (7), 665–672.

Dalvand, A., Nabizadeh, R., Ganjali, M. R., Khoobi, M., Nazmara, S. & Mahvi, A. H. 2016 Modeling of Reactive Blue 19 azo dye removal from colored textile wastewater using L-arginine-functionalized Fe_3O_4 nanoparticles: optimization, reusability, kinetic and equilibrium studies. *Journal of Magnetism and Magnetic Materials* **404**, 179–189.

Dalvand, A., Ehrampoush, M. H., Ghaneian, M. T., Mokhtari, M., Ebrahimi, A. A., Malek Ahmadi, R. & Mahvi, A. H. 2017 Application of chemical coagulation process for direct dye removal from textile wastewater. *Journal of Environmental Health and Sustainable Development* **2** (3), 333–339.

Dalvand, A., Khoobi, M., Nabizadeh, R., Ganjali, M. R., Gholibegloo, E. & Mahvi, A. H. 2018 Reactive dye adsorption from aqueous solution on HPEI-modified Fe_3O_4 nanoparticle as a superadsorbent: characterization, modeling, and optimization. *Journal of Polymers and the Environment* **26** (8), 3470–3483.

Dubinin, M. 1947 *The Equation of the Characteristic Curve of Activated Charcoal*. Paper presented at the Dokl. Akad. Nauk. SSSR.

Errais, E., Duplay, J., Darragi, F., M'Rabet, I., Aubert, A., Huber, F. & Morvan, G. 2011 Efficient anionic dye adsorption on natural untreated clay: kinetic study and thermodynamic parameters. *Desalination* **275** (1), 74–81.

Fathi, M., Asfaram, A. & Farhangi, A. 2015 Removal of Direct Red 23 from aqueous solution using corn stalks: isotherms, kinetics and thermodynamic studies. *Spectrochimica Acta Part A: Molecular and Biomolecular Spectroscopy* **135**, 364–372.

Feng, Q., Honbu, C., Yanagisawa, K., Yamasaki, N. & Komarneni, S. 2000 Synthesis of $LiAl_2(OH)_6^+$ intercalated montmorillonite by a hydrothermal soft chemical reaction. *Journal of Materials Chemistry* **10** (2), 483–488.

Freundlich, H. 1906 Over the adsorption in solution. *Journal of Physical Chemistry* **57** (385471), 1100–1107.

Ghaedi, M., Mazaheri, H., Khodadoust, S., Hajati, S. & Purkait, M. 2015 Application of central composite design for simultaneous removal of methylene blue and Pb^{2+} ions by walnut wood activated carbon. *Spectrochimica Acta Part A: Molecular and Biomolecular Spectroscopy* **135**, 479–490.

Gholami-Borujeni, F., Mahvi, A. H., Nasseri, S., Faramarzi, M. A., Nabizadeh, R. & Alimohammadi, M. 2011 Enzymatic treatment and detoxification of acid orange 7 from textile wastewater. *Applied Biochemistry and Biotechnology* **165** (5–6), 1274–1284.

Gopal, N., Asaithambi, M., Sivakumar, P. & Sivakumar, V. 2014 Adsorption studies of a direct dye using polyaniline coated activated carbon prepared from *Prosopis juliflora*. *Journal of Water Process Engineering* **2**, 87–95.

Hassan, A., Abdel-Mohsen, A. & Fouda, M. M. 2014 Comparative study of calcium alginate, activated carbon, and their composite beads on methylene blue adsorption. *Carbohydrate Polymers* **102**, 192–198.

Hebeish, A., Ramadan, M., Abdel-Halim, E. & Abo-Okeil, A. 2011 An effective adsorbent based on sawdust for removal of direct dye from aqueous solutions. *Clean Technologies and Environmental Policy* **13** (5), 713–718.

Ho, Y. S. & McKay, G. 1998 Sorption of dye from aqueous solution by peat. *Chemical Engineering Journal* **70** (2), 115–124.

Jamshidi, A., Rafiee, M. & Rad, M. J. 2014 Adsorption behavior of reactive blue 29 dye on modified nanoclay. *Trends in Applied Sciences Research* **9** (6), 303.

Kaygusuz, H., Çoşkunırmak, M. H., Kahya, N. & Erim, F. B. 2015 Aluminum alginate–Montmorillonite composite beads for defluoridation of water. *Water, Air, & Soil Pollution* **226** (1), 1–9.

Khazaei, M., Nasseri, S., Ganjali, M. R., Khoobi, M., Nabizadeh, R., Gholibegloo, E. & Nazmara, S. 2018 Selective removal of lead ions from aqueous solutions using 1, 8-dihydroxyanthraquinone (DHAQ) functionalized graphene oxide; isotherm, kinetic and thermodynamic studies. *RSC Advances* **8** (11), 5685–5694.

Kizilkaya, B. 2012 Usage of biogenic apatite (Fish bones) on removal of basic fuchsin dye from aqueous solution. *Journal of Dispersion Science and Technology* **33** (11), 1596–1602.

Konicki, W., Pełech, I., Mijowska, E. & Jasińska, I. 2012 Adsorption of anionic dye Direct Red 23 onto magnetic multi-walled carbon nanotubes-fe$_3$c nanocomposite: kinetics, equilibrium and thermodynamics. *Chemical Engineering Journal* **210**, 87–95.

Kooh, M. R. R., Dahri, M. K. & Lim, L. B. L. 2018 Jackfruit seed as low-cost adsorbent for removal of malachite green: artificial neural network and random forest approaches. *Environmental Earth Sciences* **77** (12), 434.

Kubilay, Ş., Gürkan, R., Savran, A. & Şahan, T. 2007 Removal of Cu (II), Zn (II) and Co (II) ions from aqueous solutions by adsorption onto natural bentonite. *Adsorption* **13** (1), 41–51.

Lagergren, S. K. 1898 About the theory of so-called adsorption of soluble substances. *Sven. Vetenskapsakad. Handingarl* **24**, 1–39.

Langmuir, I. 1916 The constitution and fundamental properties of solids and liquids. *Part I. Solids. Journal of the American Chemical Society* **38** (11), 2221–2295.

Magdy, Y. & Altaher, H. 2018 Kinetic analysis of the adsorption of dyes from high strength wastewater on cement kiln dust. *Journal of Environmental Chemical Engineering* **6** (1), 834–841.

Mahmoodi, N. M. & Dalvand, A. 2013 Treatment of colored textile wastewater containing acid dye using electrocoagulation process. *Desalination and Water Treatment* **51** (31–33), 5959–5964.

Mahmoodi, N. M. & Masrouri, O. 2015 Cationic dye removal ability from multicomponent system by magnetic carbon nanotubes. *Journal of Solution Chemistry* **44** (8), 1568–1583.

Mahmoodi, N. M., Salehi, R., Arami, M. & Bahrami, H. 2011 Dye removal from colored textile wastewater using chitosan in binary systems. *Desalination* **267** (1), 64–72.

Mahmoodi, N. M., Masrouri, O. & Arabi, A. M. 2014 Synthesis of porous adsorbent using microwave assisted combustion method and dye removal. *Journal of Alloys and Compounds* **602**, 210–220.

Mahvi, A. H. 2008 Application of agricultural fibers in pollution removal from aqueous solution. *International Journal of Environmental Science & Technology* **5** (2), 275–285.

Mahvi, A. H., Ghanbarian, M., Nasseri, S. & Khairi, A. 2009 Mineralization and discoloration of textile wastewater by TiO_2 nanoparticles. *Desalination* **239** (1), 309–316.

Maleki, A., Mahvi, A. H., Ebrahimi, R. & Zandsalimi, Y. 2010 Study of photochemical and sonochemical processes efficiency for degradation of dyes in aqueous solution. *Korean Journal of Chemical Engineering* **27** (6), 1805–1810.

Min-Yu, T. & Su-Hsia, L. 2006 Removal of methyl orange dye from water onto raw and acidactivated montmorillonite in fixed beds. *Desalination* **201**, 71–81.

Moharami, S. & Jalali, M. 2013 Removal of phosphorus from aqueous solution by Iranian natural adsorbents. *Chemical Engineering Journal* **223**, 328–339.

Niroumand, H., Zain, M. & Alhosseini, S. N. 2013 The influence of nano-clays on compressive strength of earth bricks as sustainable materials. *Procedia-Social and Behavioral Sciences* **89**, 862–865.

Öztürk, A. & Malkoc, E. 2014 Adsorptive potential of cationic Basic Yellow 2 (BY2) dye onto natural untreated clay (NUC) from aqueous phase: mass transfer analysis, kinetic and equilibrium profile. *Applied Surface Science* **299**, 105–115.

Palamthodi, S. & Lele, S. 2016 Optimization and evaluation of reactive dye adsorption on bottle gourd peel. *Journal of Environmental Chemical Engineering* **4** (4), 4299–4309.

Ratnamala, G., Shetty, K. V. & Srinikethan, G. 2012 Removal of remazol brilliant blue dye from dye-contaminated water by adsorption using red mud: equilibrium, kinetic, and thermodynamic studies. *Water, Air, & Soil Pollution* **223** (9), 6187–6199.

Salam, M. A., Kosa, S. A. & Al-Beladi, A. A. 2017 Application of nanoclay for the adsorptive removal of Orange G dye from aqueous solution. *Journal of Molecular Liquids* **241**, 469–477.

Shirmardi, M., Mahvi, A. H., Hashemzadeh, B., Naeimabadi, A., Hassani, G. & Niri, M. V. 2013 The adsorption of malachite green (MG) as a cationic dye onto functionalized multi walled carbon nanotubes. *Korean Journal of Chemical Engineering* **30** (8), 1603–1608.

Si, J., Yuan, T. Q. & Cui, B. K. 2015 Exploring strategies for adsorption of azo dye Congo Red using free and immobilized biomasses of *Trametes pubescens*. *Annals of Microbiology* **65** (1), 411–421.

Soleimani, M. & Siahpoosh, Z. H. 2015 Ghezeljeh nanoclay as a new natural adsorbent for the removal of copper and mercury ions: equilibrium, kinetics and thermodynamics studies. *Chinese Journal of Chemical Engineering* **23** (11), 1819–1833.

Tan, L., Jain, K. & Rozaini, C. 2010 Adsorption of textile dye from aqueous solution on pretreated mangrove bark, an agricultural waste: equilibrium and kinetic studies. *Journal of Applied Sciences in Environmental Sanitation* **5**, 3.

Vu, A. T., Xuan, T. N. & Lee, C. H. 2019 Preparation of mesoporous $Fe_2O_3 \cdot SiO_2$ composite from rice husk as an efficient heterogeneous Fenton-like catalyst for degradation of organic dyes. *Journal of Water Process Engineering* **28**, 169–180.

Weber, W. J. & Morris, J. C. 1963 Kinetics of adsorption on carbon from solution. *Journal of the Sanitary Engineering Division* **89** (2), 31–60.

Weber, C. T., Collazzo, G. C., Mazutti, M. A., Foletto, E. L. & Dotto, G. L. 2014 Removal of hazardous pharmaceutical dyes by adsorption onto papaya seeds. *Water Science & Technology* **70** (1), 102–107.

Yan, W., Hanjin, L., Hou, W., Can, W., Jian, Z. & Zilong, Z. 2013 Adsorption of hexavalent chromium from aqueous solutions by graphene modified with cetyltrimethylammonium bromide. *Journal of Colloid and Interface Science* **394**, 183–191.

Yousefi, N., Nabizadeh, R., Nasseri, S., Khoobi, M., Nazmara, S. & Mahvi, A. H. 2017 Decolorization of direct blue 71 solutions using tannic acid/polysulfone thin film nanofiltration composite membrane; preparation, optimization and characterization of anti-fouling. *Korean Journal of Chemical Engineering* **34** (8), 2342–2353.

Yuan, G. & Wu, L. 2007 Allophane nanoclay for the removal of phosphorus in water and wastewater. *Science and Technology of Advanced Materials* **8** (1–2), 60.

Yuliani, G., Garnier, G. & Chaffee, A. L. 2017 Utilization of raw and dried Victorian brown coal in the adsorption of model dyes from solution. *Journal of Water Process Engineering* **15**, 43–48.

Zarei, H., Nasseri, S., Nabizadeh, R., Shemirani, F., Dalvand, A. & Mahvi, A. H. 2017 Modeling of arsenic removal from aqueous solution by means of MWCNT/alumina nanocomposite. *Desalination and Water Treatment* **67**, 196–205.

First received 25 May 2019; accepted in revised form 26 September 2019. Available online 11 October 2019